Developmental Biology 458 (2020) 246–256

Contents lists available at ScienceDirect

Developmental Biology

journal homepage: www.elsevier.com/locate/developmentalbiology

Six2 regulates Pax9 expression, palatogenesis and craniofacial bone formation

Yan Yan Sweat [a], Mason Sweat [a], Maurisa Mansaray [a], Huojun Cao [b,c], Steven Eliason [a], Waisu L. Adeyemo [d], Lord J.J. Gowans [e], Mekonen A. Eshete [f], Deepti Anand [h], Camille Chalkley [a], Irfan Saadi [g], Salil A. Lachke [h,i], Azeez Butali [c,j], Brad A. Amendt [a,c,*]

[a] Department of Anatomy and Cell Biology and the Craniofacial Anomalies Research Center, The University of Iowa, Iowa City, IA, 52242, USA
[b] Department of Endodontics, College of Dentistry, The University of Iowa, Iowa City, IA, 52242, USA
[c] Iowa Institute of Oral Health Research, University of Iowa, Iowa City, IA, 52242, USA
[d] Department of Oral and Maxillofacial Surgery, University of Lagos, Lagos, Nigeria
[e] Kwame Nkrumah University of Science and Technology, Kumasi, Ghana
[f] Addis Ababa University, School of Public Health, Addis Ababa, Ethiopia
[g] Department of Anatomy and Cell Biology, University of Kansas Medical Center, Kansas City, KS, 66160, USA
[h] Department of Biological Sciences, University of Delaware, Newark, DE, 19716, USA
[i] Center for Bioinformatics and Computational Biology, University of Delaware, Newark, DE, 19716, USA
[j] Department of Oral Pathology, Radiology and Medicine, College of Dentistry, University of Iowa, Iowa City, IA, 52242, USA

A B S T R A C T

In this study, we investigated the role of the transcription factor *Six2* in palate development. *Six2* was selected using the SysFACE tool to predict genes from the 2p21 locus, a region associated with clefting in humans by GWAS, that are likely to be involved in palatogenesis. We functionally validated the predicted role of *Six2* in palatogenesis by showing that 22% of *Six2* null embryos develop cleft palate. *Six2* contributes to palatogenesis by promoting mesenchymal cell proliferation and regulating bone formation. The clefting phenotype in $Six2^{-/-}$ embryos is similar to *Pax9* null embryos, so we examined the functional relationship of these two genes. Mechanistically, SIX2 binds to a *PAX9* 5' upstream regulatory element and activates *PAX9* expression. In addition, we identified a human *SIX2* coding variant (p.Gly264Glu) in a proband with cleft palate. We show this missense mutation affects the stability of the SIX2 protein and leads to decreased *PAX9* expression. The low penetrance of clefting in the *Six2* null mouse combined with the mutation in one patient with cleft palate underscores the potential combinatorial interactions of other genes in clefting. Our study demonstrates that *Six2* interacts with the developmental gene regulatory network in the developing palate.

1. Introduction

Cleft lip with or without cleft palate (CL/P) is among the most common human birth defects, affecting between 1 in 500 and 1 in 2500 newborns each year, depending on the population examined (Conway et al., 2015; Dixon et al., 2011). Isolated, non-syndromic CLP (NSCL/P), a subset of CL/P, is classified in patients who exhibit clefting of the lip with or without palatal clefting that occurs without any other obvious developmental defects (Stuppia et al., 2011). NSCL/P makes up about 70% of clefting cases (Dixon et al., 2011). The complex etiology of the condition includes both environmental and genetic predisposing factors (Leslie et al., 2017). Developmental studies into the genetic underpinnings of clefting have revealed a number of genes that are required for palatogenesis. Many of these genes are transcription factors that are expressed in the neural crest derived mesenchymal tissue in the developing craniofacial region, for example *Pax9*, which is essential for palatogensesis as well as tooth morphogenesis (Peters et al., 1998; Zhou et al., 2013). More work is required to comprehensively identify all the genes which participate in the development of the palate, and to understand how they interact with each other to guide this complex process.

GWAS studies have been essential for the identification of genes that contribute to the risk of NSCL/P, and over 15 different genomic loci have been implicated to date (Birnbaum et al., 2009; Butali et al., 2018; Cox et al., 2018; Grant et al., 2009; Leslie et al., 2016; Ludwig et al., 2012; Mangold et al., 2010; Sun et al., 2015; Wolf et al., 2015; Yu et al., 2017). After genomic loci are identified, studies must be employed to identify functional variants that are causative for clefting. Several of these studies have been successfully performed to date (Leslie et al., 2015; Liu et al.,

* Corresponding author. University of Iowa, Carver College of Medicine, Craniofacial Anomalies Research Center, 1-675 BSB, 51 Newton Rd, Iowa City, IA, 52242, USA
E-mail address: brad-amendt@uowa.edu (B.A. Amendt).

https://doi.org/10.1016/j.ydbio.2019.11.010
Received 16 August 2019; Received in revised form 30 October 2019; Accepted 15 November 2019
Available online 23 November 2019

Table 1
Primers used in the manuscript.

ChIP Primers				
Negative control	F	5′	CCTGGTTTGTTCCCACTATAGTG	3′
	R	5′	GCGCGCTCTCAGAGCATC	3′
SIX2 BS	F	5′	GCGACTCCGACGCTAACCC	3′
	R	5′	AGCTGCGTTTCCAGCCTG	3′
qRT-PCR Primers				
SIX2	F	5′	AGGCCAAGGAAAGGGAGAAC	3′
	R	5′	GAGCTGCCTAACACCGACTT	3′
β-actin	F	5′	CTCTTCCAGCCTTCCTTC	3′
	R	5′	ATCTCCTTCTGCATCCTGTC	3′

2017; Rahimov et al., 2008; Zhang et al., 2015). However, more work is required to streamline the identification and functional validation of variants found within genomic loci implicated by GWAS studies. In this work, we use a new approach, the web-based tool SysFACE (Systems tool for craniofacial expression-based gene discovery), to identify high-priority candidate genes for palate development from regions identified by GWAS, and confirmed this prediction by functional analysis *in vivo* and *in vitro* (Liu et al., 2017). This systen has been used to identify candidate genes in eye development (Kakrana et al., 2018).

Previous reports have indicated a role for *Six2* in craniofacial development, but these efforts did not identify or examine the etiology of clefting in *Six2*$^{-/-}$embryos and mice (He et al., 2010; Liu et al., 2019; Okello et al., 2017). In the present study, we observed that 22% of *Six2*$^{-/-}$ embryos examined had oral clefts. This re-examination of the *Six2*$^{-/-}$ mouse line was prompted by the SysFACE tool, which identified *Six2* as a relevant transcription factor for craniofacial development because it is highly expressed and enriched in craniofacial tissues at different developmental stages when palatogenesis is occurring. Further, we find that a role for human *SIX2* in clefting is also evident from the enrichment of a variant *SIX2 (p.Gly264Glu)* in a cleft palate patient, compared with control populations.

There are six members in the sine *oculus (Six) family* named *Six1-Six6* (Nonomura et al., 2010). In humans, *SIX1* and *SIX2* regulate one another to control nephrogenesis (O'Brien et al., 2016). Each of the six members in the *Six* family has a DNA-binding homeodomain (HD) and a Six domain, which contributes to the DNA binding and protein-protein interaction function. There are three homologous C-termini shared among the *Six* family members, allowing the division of the proteins into groups (*Six1/2, Six 3/6, and Six 4/5*) (Brodbeck et al., 2004; Kawakami et al., 1996).

The deletion of *SIX2* in humans causes frontonasal dysplasia syndrome, suggesting a role for *SIX2* in craniofacial development (Hufnagel et al., 2016). *Six2*$^{-/-}$ mice die shortly after birth. *Six2* also has been found to play an important role in kidney development. In undifferentiated nephron progenitors, a Six2/Lef/Tcf complex prevents the expression of targets to maintain progenitor self-renewal. In differentiating nephron progenitor cells, *Six2* expression is diminished and *β-catenin* expression is increased, initiating Wnt target gene transcription including *Fgf8* and *Wnt 4* (Park et al., 2012). However, the function of *Six2* in palatogenesis is not well studied.

It is known that *Pax9* regulates palatogenesis through Bmp, Fgf and Shh signaling; knocking out *Pax9* causes decreased cell proliferation in mouse palatal shelves (Kist et al., 2005; Peters et al., 1998; Zhou et al., 2013). Recently, *Pax9* has also been reported to regulate Wnt signaling in palate development by directly regulating the transcription of *Dkk1* and *Dkk2* (Jia et al., 2017). Both *Six2* and *Pax9* are expressed on the palatal mesenchyme at E13.5 (Jia et al., 2017; Okello et al., 2017). However, little is known about the regulation between *Six2* and *Pax9* during palatal development. In our study, we found *PAX9* is a target of *SIX2*. We further show that SIX2 directly binds to the *PAX9* upstream promoter and activates *PAX9* expression.

	SysFACE expression						SysFACE enrichment					
	Six2	*Epcam*	*Eml4*	*Prkce*	*Msh2*	*Six3*	*Six2*	*Epcam*	*Eml4*	*Prkce*	*Msh2*	*Six3*
E10.0 Mandible	201.0	1319.2	1644.8	198.9	1780.0	85.4	-1.8	2.3	1.7	1.1	1.2	-2.3
E10.5 Mandible	295.7	881.4	1099.0	160.5	876.2	96.9	-1.3	1.5	1.1	-1.2	-1.7	-2.0
E10.5 Mandible (lateral)	500.2	564.0	1463.0	134.3	1785.8	93.7	1.4	1.0	1.5	-1.4	1.2	-2.1
E10.5 Mandible (medial)	298.4	989.4	1313.7	165.7	1724.5	82.3	-1.2	1.8	1.4	-1.1	1.2	-2.4
E11.0 Mandible	648.0	794.1	1260.6	181.7	1291.8	87.7	1.8	1.4	1.3	-1.0	-1.1	-2.2
E11.5 Mandible	967.1	548.9	1374.7	225.1	1059.4	94.5	2.7	-1.0	1.4	1.2	-1.4	-2.1
E11.5 Mandible (medial)	373.3	639.5	1159.6	246.0	1545.8	81.3	1.0	1.1	1.2	1.3	1.0	-2.4
E12.0 Mandible	948.8	712.5	1389.7	233.7	1185.5	88.8	2.6	1.3	1.4	1.2	-1.3	-2.2
E12.5 Mandible	679.8	936.6	1516.2	266.2	1035.5	83.0	1.9	1.7	1.5	1.4	-1.4	-2.4
E12.5 Mandible-2	474.9	1148.1	1321.6	309.6	1205.6	93.7	1.3	2.1	1.4	1.7	-1.2	-2.1
E10.5 Maxilla	611.0	824.7	1119.9	176.0	946.8	105.2	1.6	1.5	1.1	-1.1	-1.6	-1.9
E11.0 Maxilla	921.0	1064.7	1235.0	161.5	1226.4	95.8	2.5	1.9	1.3	-1.2	-1.2	-2.0
E11.5 Maxilla	1769.5	845.5	1737.5	208.2	1265.9	93.7	5.0	1.5	1.8	1.1	-1.2	-2.1
E12.0 Maxilla	1288.9	1029.1	1331.2	188.0	1077.9	95.6	3.4	1.8	1.3	1.0	-1.4	-2.0
E12.5 Maxilla	1567.5	1305.5	1808.4	313.4	1129.4	98.1	4.3	2.3	1.9	1.7	-1.3	-2.0
E10.5 Frontonasal	1142.1	1880.1	1073.4	139.6	993.9	224.4	3.2	3.3	1.1	-1.4	-1.5	1.1
E11.0 Frontonasal	1566.7	1997.2	1176.2	169.8	1363.5	182.5	4.4	3.6	1.2	-1.1	-1.1	-1.1
E11.5 Frontonasal	2224.2	1723.7	1365.9	214.0	1151.1	203.5	6.2	3.0	1.4	1.1	-1.3	1.0
E12.0 Frontonasal	2230.5	2325.6	1227.7	210.6	1256.2	170.6	6.2	4.1	1.3	1.1	-1.2	-1.1
E12.5 Frontonasal	1996.0	2436.0	1522.4	267.5	1065.8	228.3	5.5	4.3	1.6	1.4	-1.4	1.2
E13.5 Palate	881.9	2619.6	1188.4	516.3	1112.6	175.5	2.5	4.7	1.2	2.8	-1.3	-1.1
E14.5 Palate	676.0	2793.9	1039.4	412.4	849.2	184.8	1.9	5.0	1.1	2.2	-1.7	-1.1
E14.5 Palate-2	895.7	1436.0	1490.1	219.9	1017.0	154.8	2.5	2.6	1.5	1.2	-1.5	-1.3
Palate P0	117.5	3058.7	559.2	253.1	442.3	82.4	-3.3	5.0	-1.7	1.2	-3.4	-2.4

Fig. 1. SysFACE identifies *Six2* as a high-priority candidate in craniofacial development. Mouse craniofacial expression data was analyzed by SysFACE (Systems tool for craniofacial expression-based gene discovery). SysFACE analysis reveals that *Six2* has significant expression (absolute expression in fluorescent intensity units >100, $p < 0.05$) and significant enrichment (craniofacial tissue compared to whole-embryo body tissue reference dataset >1.5-fold change, $p < 0.05$) in several mouse craniofacial tissues at various embryonic stages. Other gene candidates are shown from the 2p21 analyses.

2. Materials and methods

2.1. Gene identification using SysFACE (systems tool for craniofacial expression-based gene discovery

SysFACE was used to prioritize candidate genes in the list from the GWAS meta-analysis according to their expression in craniofacial (CF) tissues. This tool has been previously applied to prioritize several important cleft palate candidate genes (Butali et al., 2018; Cox et al., 2018; Liu et al., 2017). While the tool itself will be described in detail elsewhere, in summary, SysFACE is based on a unique processing protocol of microarray-based genome-level gene CF expression profiles from publicly available resources such as FaceBase. Specifically, expression datasets from the following mouse CF tissues (Mandible, Palate, Frontonasal, and Maxillary) obtained from FaceBase (FB00000467.01, FB00000468.01, FB00000474.01) and NCBI Gene Expression Omnibus (GEO) (GSE35091, GSE7759, GSE11400, GSE31004) were analyzed. In this analysis, we estimate the enriched expression of individual genes in specific CF-tissues based on their fold-change upregulation in these tissues compared to their expression in mouse whole-embryo body (WB) tissue at E10.5, E11.5, and E12.5 (GSE32334) in an approach termed "WB *in silico* subtraction" as previously described (Anand et al., 2018,; Lachke et al., 2012). The obtained *SysFACE*-based CF-tissue enrichment as well CF-tissue expression scores are presented in a heatmap figure, created using *in-house* python script. From this analysis, we identified *Six2* as being highly expressed and enriched in specific CF tissues.

2.2. Mouse lines and embryonic staging

Mice were housed and cared for by the standards and suggestions of The Program of Embryo Resources at the University of Iowa. *Six2*$^{+/-}$ mice were obtained from Jackson Laboratories (stock number 009600). This mouse line was maintained on a C57BL/6 background. In order to time pregnancies, females from breeder cages were checked for the presence of a vaginal plug in the morning of the day after the male was introduced. Upon finding a plug, the breeding pair were separated. The day of plug observation is noted as E0.5.

2.3. Tissue fixation and slide preparation

Embryos were harvested from pregnant females on the designated day and dissected in cold 1× PBS. A non-essential tissue sample was taken for genotyping purposes. The tissues were subsequently fixed in 4% PFA (ChemCruz) for 0.5–4 h and then dehydrated through an ethanol gradient (70%–100%, each step 4 h to overnight). Tissues were precleared in xylene and embedded in paraffin. After embedding, 7 μm sections were cut using the microtome (Thermo, HM325), floated out and attached to slides (VWR VistaVision Microscope Slides). Slides used for immunofluorescence were baked no longer than 2 h at 65 °C; slides for other applications were baked overnight to affix the tissue section to the slide.

2.4. Immunofluorescence staining and confocal imaging

Slides were re-hydrated and subjected to antigen retrieval by citrate boiling for 20 min. Slides were washed 3 times with 1× PBS and blocked with 20% donkey serum (sigma, D9663A). After blocking, the primary antibody for Six2 (Proteintech, 11562-1-AP), Osx (abcam, ab22552), BrdU (Invitrogen 00–0103) was applied and incubated overnight at 4 °C. Slides were washed 3 times with 1× PBS and in a dark box, incubated with secondary antibody (Life Technologies) for 30 min at room temperature. The remainder of the procedure was carried out in the dark. Slides were washed 3 times in 1× PBS and incubated with DAPI solution (Thermo Scientific). Slides were washed 3 times in 1× PBS and a hydroseal buffer was used to mount a cover slip. Slides were dried for 1–2 h at room temperature and subjected to confocal imaging. Images were captured using the ZEISS 700 confocal microscope and Zen imaging software. The different channels were combined using ImageJ software prior to publication.

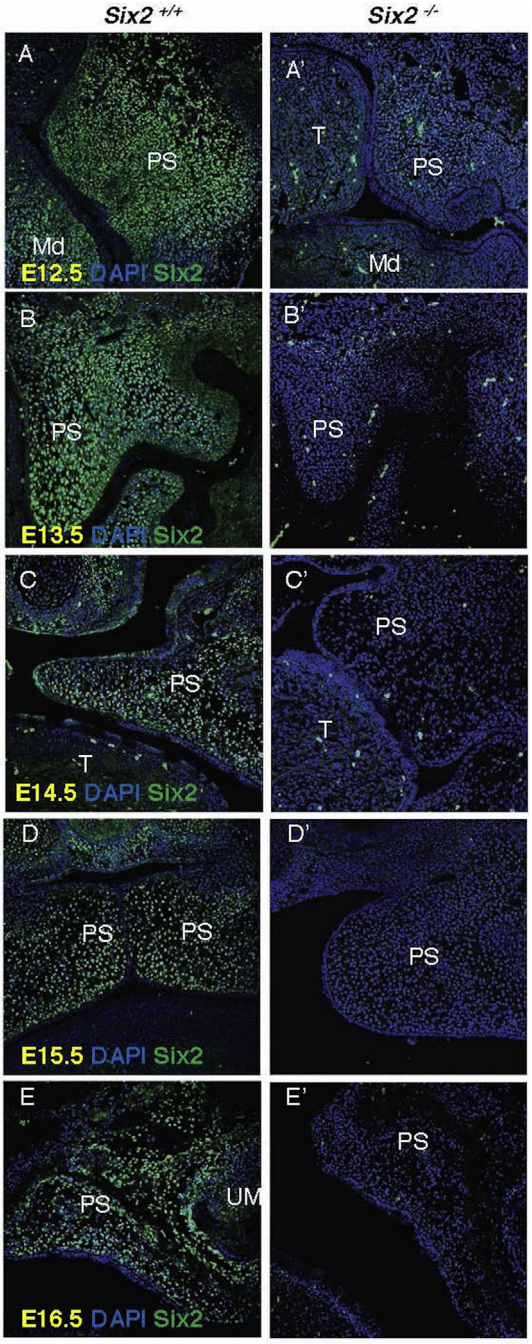

Fig. 2. Six2 is expressed in the palatal mesenchyme and undetectable in *Six2*$^{-/-}$ embryos. A-E. *Six2* is expressed in the palatal mesenchyme from E12.5 to E16.5 developmental stages. **A′-E′**. Six2 is not detectable in *Six2*$^{-/-}$ embryos at any developmental stage. PS, palate shelf; Md, mandible; T, tongue; UM, upper molar.

2.5. BrdU assay

Pregnant females were injected 2 h prior to sacrifice to label proliferative cells with BrdU (10μl/g body weight, Invitrogen 00–0103) and detected using a rat monoclonal anti-BrdU antibody (Abcam, ab6326, 1:250). Medial tip regions of the extending palatal shelves were analyzed by counting the number of BrdU + cells in a given area, represented by a

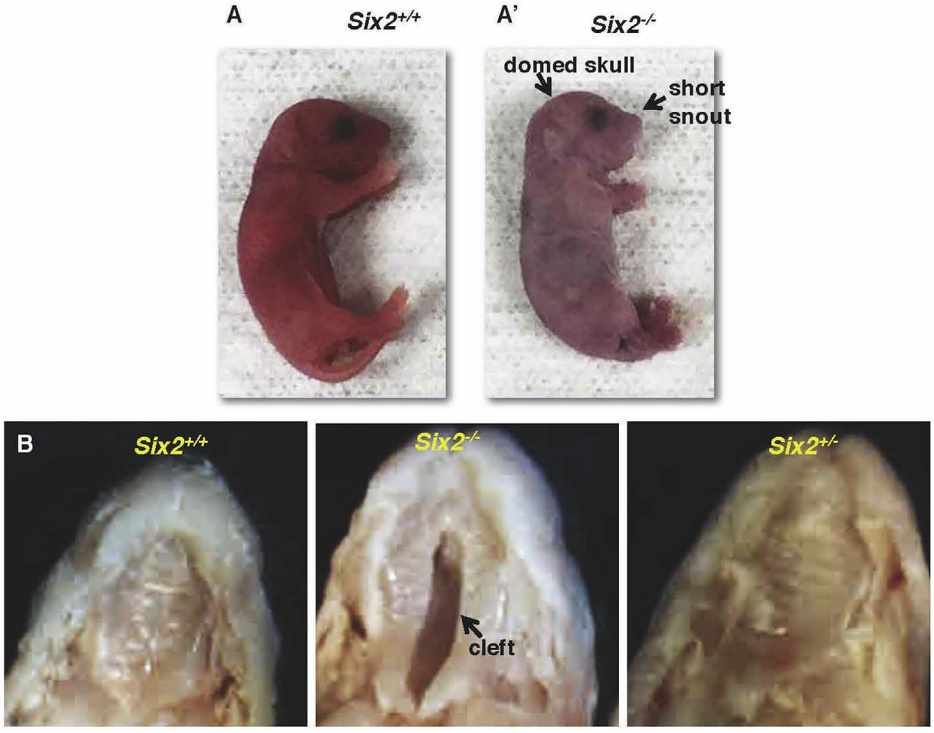

Fig. 3. ***Six2*$^{-/-}$ neonatal mice have craniofacial phenotypes. A-A'.** *Six2*$^{+/+}$and *Six2*$^{-/-}$ P0 mice were collected after birth. *Six2* $^{-/-}$ mice die and exhibit a domed skull and a short snout. **B.** Examining the palate of P0 mice revealed a cleft in the secondary palate of *Six2*$^{-/-}$ embryos.

white dotted circle.

2.6. Hematoxylin and eosin staining

Slides were de-parrafinized and rehydrated using a reverse ethanol gradient. After rehydration, slides were incubated in Hematoxylin for 4 min. Slides were de-stained using 9 dips in 95%EtOH, 1 M HCl and bluing was carried out using 0.1% Sodium Bicarbonate for 30 s. Slides were washed in water and dehydrated in an ethanol gradient to 95% EtOH and stained in Eosin for 1 min. Images were taken using an inverted Nikon microscope.

2.7. Whole skeletal staining

Skin and internal organs were removed from P0 mice. The mice were scalded in 65 °C H_2O to fully remove the skin. The carcass was then fixed overnight in 95% EtOH. Alcian Blue staining proceeded overnight (800 ml 95% EtOH, 200 ml acetic acid, Alcian Blue 8GX sigma A3175 150 mg. Carcasses were washed in 95% EtOH for 5 h and cleared using 2% KOH. A final dissection step was then performed to remove the remaining fat and skin. Alizarin red staining (1% KOH, 0.015% Alizarin red Sigma A3757) staining was performed overnight. Sections were cleared for an additional 3 days in 1%KOH, 20% glycerol for 3 days, and stored in 1:1 glycerol and 95% EtOH. Images were taken using a dissecting microscope.

2.8. Alizarin red staining of tissue sections

Slides were re-hydrated to water and stained with an alizarin red solution (Sigma, 2 g, in 100 ml H_2O PH 4.2) for 5 min. Slides were dehydrated in acetone and then in acetone-xylene, and mounted in xylene.

2.9. RT-qPCR

Total RNA was extracted using the RNeasy Mini Kit from Qiagen. Total RNA was reverse transcribed into cDNA by iScript Select cDNA Synthesis kit (BioRad). cDNAs were used in qPCR assays and loading was adjusted by measuring the housekeeping β-actin gene. The Real-time PCR was performed with different probes (Table 1).

2.10. ChIP

The ChIP protocol was modified from our previous publication (Sun et al., 2016) to detect interactions of the Six2 protein with chromatin. The primers used for ChIP assay are listed in Table 1.

2.11. DNA extraction and primer design

Saliva samples were collected using the Oragene DNA collection kits (http://www.dnagenotek.com) from participants in Ghana, Ethiopia and Nigeria after ethical approval at all the recruitment sites. We used the optimized Oragene saliva processing protocol available in the Butali laboratory to extract DNA from both saliva and cheek swab samples. Then, we determined the concentration of double stranded DNA in each DNA sample using Quibit Assay and Quibit 2.0 Fluorometer (http://www.invitrogen.com/site/us/en/home/brands/Product-Brand/Qubit.html). Quality control for all samples was also done by checking the gender of each sample by conducting XY-genotyping using Taqman Assay kits and real time PCR.

We designed two primer sets to cover the two coding exons and the untranslated (UTRs) 5′ and 3' of *SIX2* gene. Primers were designed with Primer 3 software (http://biotools.umassmed.edu/bioapps/primer3_www.cgi) and UCSC genome browser (https://genome.ucsc.edu/) to ascertain whether these primer sets annealed to the targeted genomic region. Primer sets were designed based on *SIX2* Ref Seq number NM_016932 of genome assembly number GRCh37/hg19, 2009 (http://genome.ucsc.edu). Gradient PCR was performed to determine the annealing temperatures of each of the primer sets. Before DNA sequencing, we amplified the coding exon of *SIX2* using initial PCR. A 9 μl of master mix (comprising 10× NH_4 buffer, 5% DMSO, 200 μM DNTPs,

50 μM MgCl, water, 20 μM of forward and reverse primers as well as 5 U/μl Taq polymerase) was added to 1 μl of each DNA sample at a concentration of 4 ng/μl. In addition to the case samples on each 96-well PCR plate, 2 HAPMAP Yoruba and two water samples were added to each plate to serve as template and non-template controls respectively. A total of 270 samples were sequenced. The PCR conditions and primer sequences are available from the Butali laboratory upon request.

The success of the initial PCR was confirmed by running part of the PCR product on 2% agarose gel and size markers at 100 A and 220 V for 20 min. All gel electrophoretic products were viewed using ultraviolet light. Successful initial PCR products were shipped to Functional Biosciences, Madison, Wisconsin (http://order.functionalbio.com/seq/index) for sequencing using the ABI 3730XL DNA sequencer.

2.12. Bioinformatics analyses of DNA sequence results

Chromatograms generated from the DNA sequence data was transferred to a Unix workstation and the bases were called using PHRED (v. 0.961028) (www.phrap.org/phredphrapconsed.html). All sequences were assembled to form the contigs using PHRAP (v. 0.960731), scanned with POLYPHRED (v. 0.970312), and viewed with CONSED (v. 4). We aligned variants to human genome assembly number GRCh37/hg19, 2009 (http://genome.ucsc.edu) to ascertain the genomic location or coordinates of variants. Novel variants are those not reported in 1000 Genomes (http://www.1000genomes.org/), Exome Aggregation Consortium (ExAC) (http://exac.broadinstitute.org/), gnomad and Exome Variant Server (EVS) (http://snp.gs.washington.edu/EVS/) databases as well as literature on orofacial clefts. We carried out segregation analyses by sequencing DNA from relatives of individuals with the novel or rare variants (MAF<1%) to ascertain whether these variants were limited to cases or if they were inherited from a parent. Functional effects of identified variants on SIX2 was predicted using in-*silico* bioinformatics tools such as polyphen 2 (http://genetics.bwh.harvard.edu/pph2/) (Adzhubei et al., 2010), SIFT (http://sift.jcvi.org/) (Kumar et al., 2009) and HOPE (http://www.cmbi.ru.nl/hope) (Venselaar et al., 2010).

2.13. Statistical analysis for experiments

For each condition, three experiments were performed and the results are presented as the mean ± SEM. The differences between two groups of conditions were analyzed using an independent, two-tailed *t*-test.

3. Results

3.1. Six2 is identified as a high-priority candidate in craniofacial development by SysFACE

We mined the GWAS significant loci reported in the first meta-analysis for cleft lip with or without cleft palate (Ludwig et al., 2012). This meta-analysis data was from two previous GWAS (Beaty et al., 2010; Mangold et al., 2010). The bioinformatics resource Systems tool for craniofacial expression-based gene discovery (SysFACE) was used to prioritize potential cleft-linked candidate genes. We used SysFACE to analyze gene expression in craniofacial tissues-maxilla, mandible, frontonasal and palate (Fig. 1). This analysis showed that *Six2* exhibits high expression in craniofacial tissues-maxilla, frontonasal and palate. Furthermore, *Six2* showed enriched expression (fold change difference of individual craniofacial tissues compared to the whole embryo body reference dataset – please see methods for details) at various embryonic developmental stages, which suggests a potential function in craniofacial morphogenesis (Fig. 1).

3.2. Six2 is highly expressed during embryonic stages of palate development and Six2 null mice have cleft palate

To test the SysFACE prediction, we next carefully examined *Six2* expression during palatal development using immunofluorescence to detect *Six2* expressing cells at E12.5, E13.5, E14.5, E15.5 and E16.5 embryonic stages. We found that *Six2* was highly expressed in the developing palatal shelves at different developmental stages (Fig. 2A–E). *Six2* was highly expressed at the E12.5 and E13.5 stages of palate shelf (PS) development, and expressed at lower levels in E16.5 palatal mesenchyme. We stained for Six2 expression in *Six2*$^{-/-}$ embryos (Fig. 2A'-E') and did not detect Six2 expression in the *Six2*$^{-/-}$ embryos confirming successful knockout of *Six2*.

Six2 is associated with nephrogenesis and craniofacial development and is expressed during palatogenesis, but *Six2*$^{-/-}$ mice had not been shown to develop oral clefts (He et al., 2010; Okello et al., 2017; Self et al., 2006). The *Six2*$^{-/-}$ mice die shortly after birth at P0. These mice exhibit several craniofacial defects, including a domed skull and a short

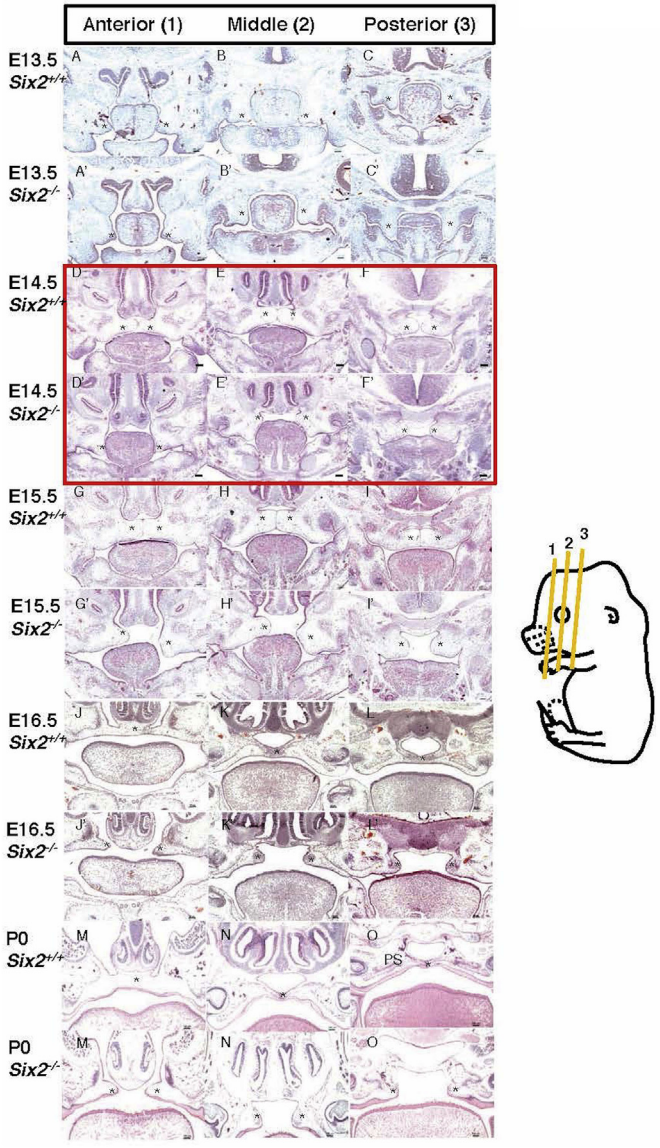

Fig. 4. *Six2*$^{-/-}$ embryos develop cleft palate. A-C. WT embryo coronal sections at E13.5. **A′-C′**. *Six2*$^{-/-}$ coronal sections at E13.5. **D-F.** WT craniofacial morphology at E14.5. **D′-F′**. *Six2*$^{-/-}$ palate shelves fail to elevate at E14.5. **G-I.** WT craniofacial morphology at E15.5. **G′-I′**. *Six2*$^{-/-}$ palate shelves fail to extend to the midline. **J-L.** WT palate formation is complete at E16.5. **J′-L′**. *Six2*$^{-/-}$ embryos have cleft palate at E16.5. **M-O.** WT palates are well formed in P0 mice. **M′-O′**. *Six2*$^{-/-}$ mice have cleft palate at P0. Scale Bars, 100 μm. 1, mouse embryos' anterior region; 2, mouse embryos' medial region; 3, mouse embryos' posterior region.

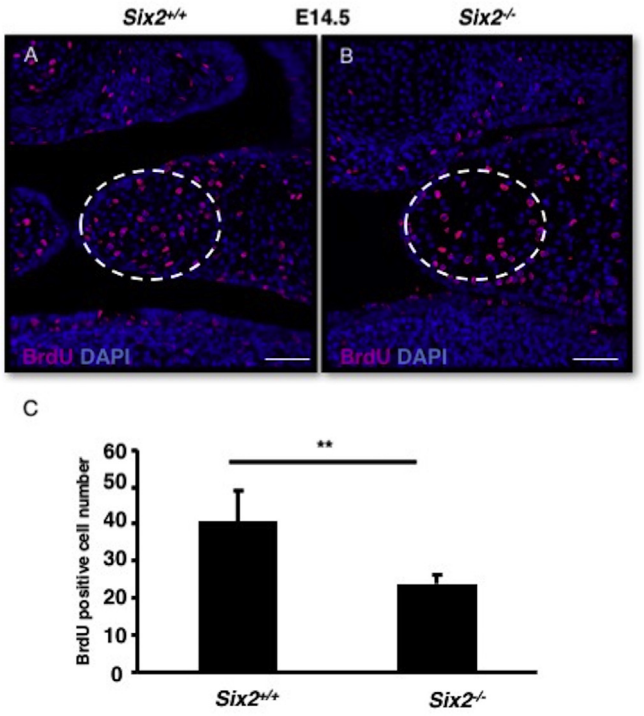

Fig. 5. *Six2*$^{-/-}$ embryos have decreased mesenchymal cell proliferation in palate shelves at E14.5. A. In order to label dividing cells, BrdU was injected into an E14.5 stage pregnant female and embryos were harvested 2 h later. Immunostaining was used to label BrdU^{+} cells on the palate shelves of WT and *Six2*$^{-/-}$ embryos. **C.** The number of proliferative cells found in E14.5 WT and *Six2*$^{-/-}$ palate mesenchyme were counted, and a statistically significant decrease in proliferation was observed in the *Six2*$^{-/-}$. Scale Bars, 50 μm. Error bars show SEM. **: *p*-values<0.01.

snout (Fig. 3A, A'), consistent with previous reports (He et al., 2010). Gross examination of a large number of *Six2*$^{-/-}$ embryos was performed during palatal development (n = 183 from E15.5-E18.5), and 22% of *Six2*$^{-/-}$ embryos were found to exhibit cleft palate (Fig. 3B).

Palate development starts from E11.5 to E17, and includes outgrowth, elevation, extension and fusion (Bush and Jiang, 2012). In order to determine which processes of palate development were defective in *Six2*$^{-/-}$ mice, we examined palate development at different embryonic stages (Fig. 4). Embryos were sectioned (coronal) and H&E staining used to examine palate formation. In wildtype (WT) embryos, the palate develops through a series of stages that begins with the outgrowth of the palatal shelves (E13.5), which occurred normally in WT and *Six2*$^{-/-}$ embryos. The clefting phenotype of the *Six2*$^{-/-}$ embryos becomes evident at E14.5 when palate shelf elevation is delayed (Fig. 4D–F, D′-F′) compared with WT embryos. At E15.5, the palate shelves have extended in WT embryos and made contact with each other forming the mid-epithelial seam (Fig. 4G–I). In *Six2*$^{-/-}$ embryos at E15.5, the process of palate shelf elevation has not been completed (Fig. 4G'-I′). In WT embryos, palate shelves are fused with each other at E16.5 and the mid-epithelial seam is lost; the mesenchymal tissues of the left and right palate shelves are merged (Fig. 4J-O). In the *Six2*$^{-/-}$ embryos, the palate shelves fail to extend at E16.5, creating a cleft at this stage and later stages (Fig. 4J'-O′).

3.3. *Six2* promotes mesenchymal cell proliferation in the early stages of palate development

We sought to determine the mechanism resulting in the failure of palate shelf extension. We reasoned that the shorter length of the palate shelves might be a direct result of a defect in cell proliferation. To test the hypothesis, BrdU was injected into pregnant mice 2 h before sacrificing to harvest E14.5 embryos. Subsequently, BrdU immunofluorescence staining was performed (Fig. 5). Interestingly a decrease in BrdU positive cells in the medial tip portion of *Six2*$^{-/-}$ palate shelves (approximately 17% reduction, P < 0.01, n = 3), compared with WT, was identified through quantifying the proliferating BrdU positive cells (Fig. 5C). E14.5

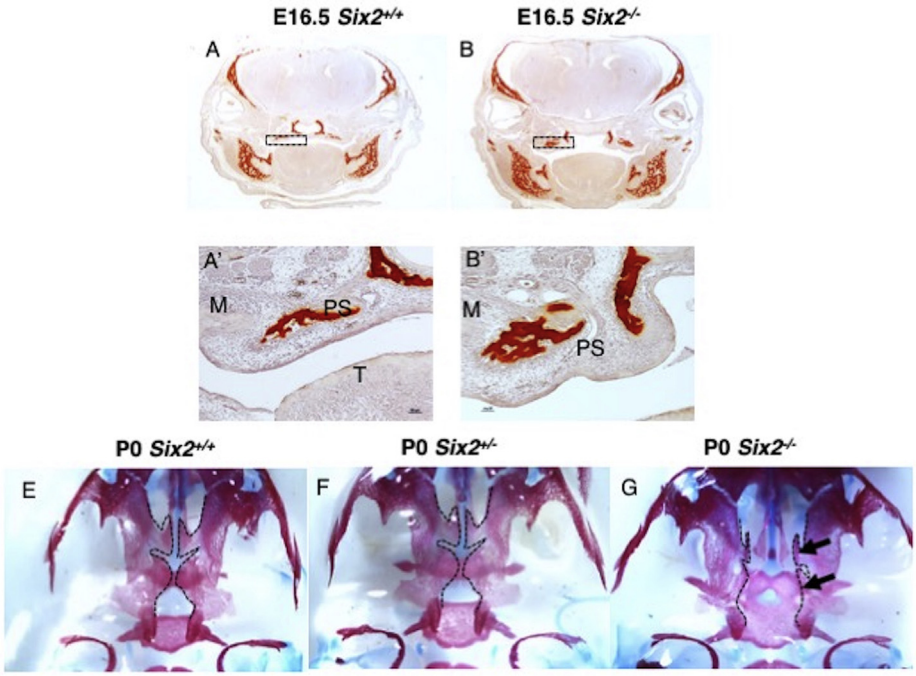

Fig. 6. An increase in ossification accompanies defective palatine bone formation in *Six2*$^{-/-}$ embryos and mice. A-B. An increase in alizarin red staining demonstrates an increase in ossification in E16.5 *Six2*$^{-/-}$ embryos compared to the WT. **A′-B′**. A magnification of the boxed regions in A and B. **E-G.** The inferior view of the oral cavity. Arrows point to the malformation of the maxillary process and abnormal palatine bone in *Six2*$^{-/-}$ mice. PS, palate shelf; M, maxilla; T, tongue.

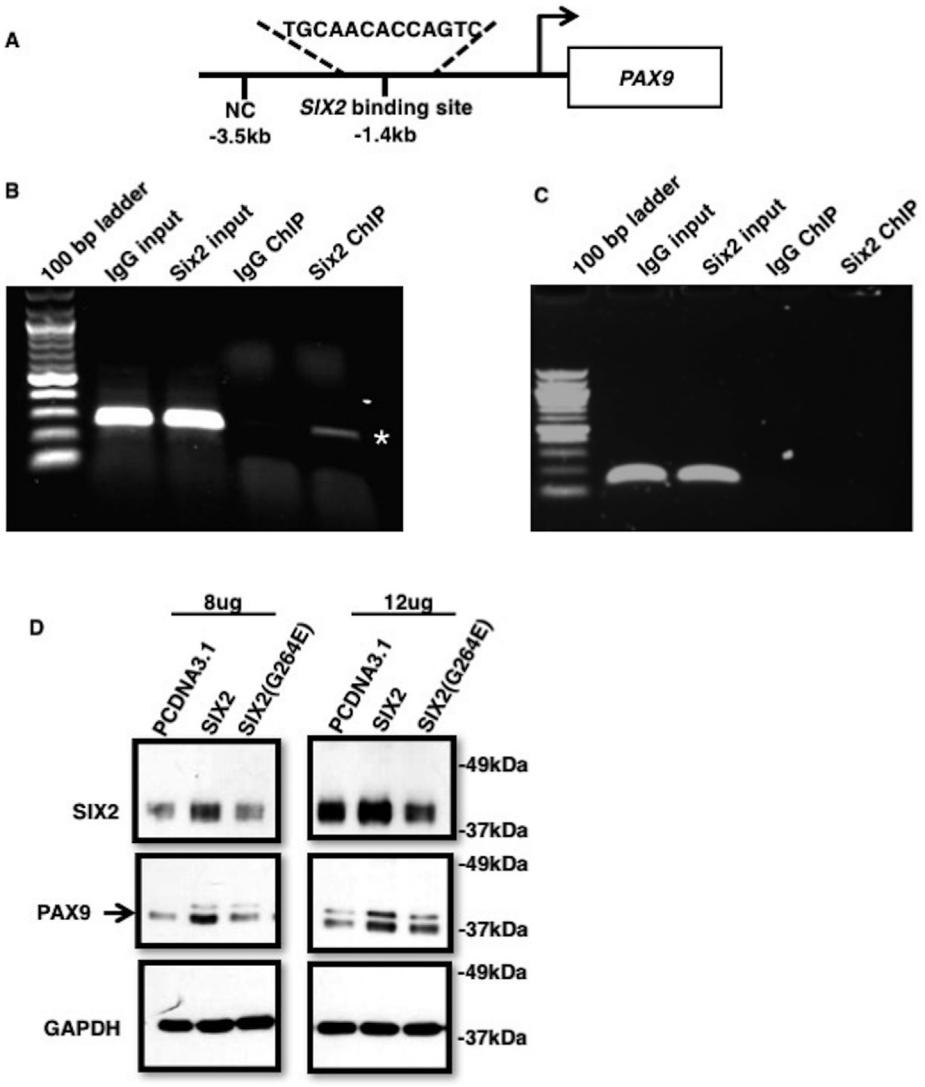

Fig. 7. SIX2 binds the *PAX9* promoter to directly promote *PAX9* expression. A. A schematic of the *PAX9* promoter highlighting a consensus SIX2 binding site and a negative control (NC) region lacking a consensus SIX2 binding site. **B.** To test the identified binding site, ChIP was performed using either an antibody specific for SIX2 or a non-specific IgG in HEK293t cells. Primers flanking the SIX2 binding site were used to successfully amplify a product from input chromatin used in ChIP reactions as well as from chromatin isolated from SIX2 ChIP, but failed to amplify a product from the IgG reaction. **C.** Primers flanking an NC region of the *PAX9* promoter not containing a SIX2 binding site amplified products from input samples but not from ChIP reactions. **D.** *SIX2* and *PAX9* expression were assayed by Western blot in HEPM cells overexpressing empty vector, *SIX2*, or *SIX2 (p.Gly264Glu)*.

Six2$^{-/-}$ embryos that did not exhibit cleft palate were also compared with WT using Ki67 staining to quantify cell proliferation, and no notable difference was found (Sup. Fig. 1A–B).

3.4. *Six2*$^{-/-}$ *embryos and neonate mice have defects associated with palate bone development and Six2 is a negative regulator of ossification*

The mouse secondary palate is composed of the palatine bone as well as the maxillary processes (Bush and Jiang, 2012), so we wanted to determine if the development of these ossified structures was defective in *Six2*$^{-/-}$ embryos. In order to better understand how bone development was affected in *Six2*$^{-/-}$ embryos, we used alizarin red staining to label mineralized tissue in coronal sections at E16.5 (Fig. 6). Interestingly, we saw a premature accumulation of mineralized tissue in the palate shelves of E16.5 *Six2*$^{-/-}$ embryos compared to WT (Fig. 6A–B, A′-B′). Further investigation revealed higher expression of the osteogenic differentiation markers *Osx* and *Runx2* in palate shelves isolated from E15.5 *Six2*$^{-/-}$ embryos with CP compared to WT (Sup. Fig. 2A–B), and there is an expansion of Osx protein on the palatal shelves in *Six2*$^{-/-}$ embryos (Sup. Fig. 2C–D).

We next examined P0 skulls using alizarin red and alcian blue staining. We found that the palate formed normally in WT embryos. However, the *Six2*$^{-/-}$ palatine process of the maxilla and palatine bone failed to extend to the midline, forming a mineralized structure on each non-extended palate (Fig. 6E–G). Taken together, these results demonstrate *Six2* is involved with regulating the ossification of the palatal mesenchyme and deleting *Six2* results in premature ossification of the maxillary process and palatine bone.

Interestingly, the increase in ossification we observed in *Six2*$^{-/-}$ embryos was specific for those with cleft palate. We examined WT and *Six2*$^{-/-}$ E17.5 embryos and found no difference in the amount of ossification of the palate shelves (Sup. Fig. 3).

3.5. *SIX2 binds the PAX9 promoter and directly regulates PAX9 expression*

Pax9$^{-/-}$ mice have similar clefting phenotypes with *Six2*$^{-/-}$ mice, and these genes are co-expressed in the palatal mesenchyme at E13.5 (Zhou et al., 2013), suggesting these genes are involved in a common pathway. These genes are co-expressed in the developing palatal mesenchyme, and the ablation of *Six2* results in decreased *Pax9* expression (Sup. Fig. 4), suggesting that *Six2* may directly regulate *Pax9* expression. The SIX2 binding motif has been previously identified, so we examined the *PAX9* promoter for the potential interaction with SIX2 (Park et al., 2012) and discovered a potential SIX2 binding site closely resembling the consensus binding sequence (Fig. 7A).

In order to test the potential SIX2 binding site for functionality, a ChIP

A

HGVS	HGVp	Type	1KG	EVS	gnomAD	ExAC	P	S
rs146753226G>A	p.Gly264Glu	Missense	0	0	0.00013	0.00013	B	T

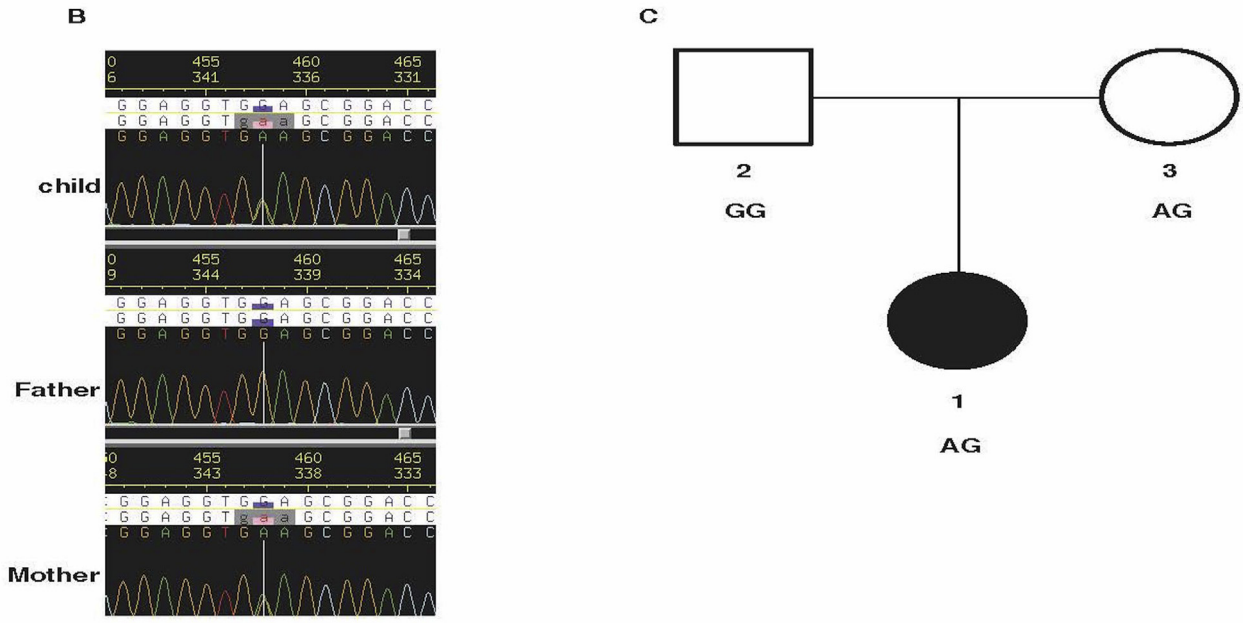

Fig. 8. Family pedigree and individual with a human *SIX2* variant. The figure shows the pedigree of the family and segregation of the *p. Gly264Glu SIX2* variant inherited by the affected child from an unaffected mother. **A**. Shows the chromatograms with nucleotide changes in the affected child, as well as the mother and father. The mother and child both carry the risk allele. **B–C.** Shows the pedigree of the family and segregation of the *p. Gly264Glu SIX2* variant inherited by the affected child from an unaffected mother. HGVS= Human genome variation society, g = genomic reference sequence, p = protein level, 1 kg = 1000 genomes, EVS = Exome variant server, ExAC = Exome aggregate consortium, P= Polyphen (B-benign) and S= Sift (T-tolerated).

assay using IgG or a SIX2 antibody was performed in HEK293t cells, which endogenously express SIX2. Primers flanking the SIX2 binding site on the *PAX9* promoter were used to amplify chromatin resulting from inputs and from each ChIP reaction. Another set of primers which do not flank a potential SIX2 binding site were designed as a negative control. PCR was performed using the two sets of primers to determine the enrichment of chromatin in the ChIP sample (Fig. 7B–C). The *SIX2* binding site ChIP PCR product was amplified and indicated by an asterisk (Fig. 7B). The negative control primers did not amplify a detectable product (Fig. 7C). Therefore, SIX2 is enriched in the *PAX9* promoter region containing the *SIX2* binding site, but not in the region lacking the binding site.

To verify the regulation of *PAX9* by SIX2, Western blot was used to examine the protein level of SIX2 and PAX9. Not surprisingly, when SIX2 was overexpressed, endogenous PAX9 expression was increased as well (Fig. 7D).

3.6. Identification of the p.Gly264Glu SIX2 variant in a family with isolated cleft palate

We sequenced *SIX2* exons in 270 cases with non-syndromic CL/P from Africa (Ghana, Ethiopia and Nigeria). We identified a rare variant in patients that has a MAF of 0.00013 (16/121,358 alleles) in the ExAc database of more than 100,000 whole exomes (accessed on 10/30/2018) and gnomAD databases (37/281,676 i.e. MAF 0.00013) that was accessed on 01/14/2019. This variant was only found in African and Hispanic individuals in both databases. It is absent in 1000 genomes and EVS (Fig. 8A). The variant segregates in the family since the unaffected mother has the variant suggesting incomplete penetrance of the phenotype (Fig. 8B and C).

3.7. The SIX2 (p.Gly264Glu) variant protein is labile and unstable

The rare *SIX2* variant was identified in CL/P patients and contains a glycine to glutamate substitution in the SIX2 C-terminal domain, which has been reported to be important for transcriptional regulation (Brodbeck et al., 2004). To examine if the *SIX2 (p.Gly264Glu)* variant affects the function of SIX2, we expressed both proteins to determine their stability in cells. The RT-qPCR results show that both *SIX2* and the variant are overexpressed with similar transcript levels (Fig. 9A). We next checked the WT SIX2 and SIX2 variant protein levels by Western blotting. Both SIX2 and the SIX2 (p.Gly264Glu) are overexpressed, however the level of SIX2 (p.Gly264Glu) protein detected was much lower than the SIX2 WT protein level (Fig. 9B). Taken together, the results of these two assays suggests that the SIX2 (p.Gly264Glu) might affect protein stability (Fig. 9B). To confirm these findings, cells transfected with either the wildtype or variant *SIX2* expression plasmids were treated with actinomycin D to inhibit transcription, and the levels of *SIX2* transcripts were identified on the initial day and the following three days (Fig. 9C). Similar levels of the two transcripts were detected over the four different time points (D = days after actinomycin D treatment) and both transcript levels as well as total mRNA levels in the cells were decreased on D2 and D3 compared with D0 and D1 as expected. SIX2 protein levels were also measured at the four time points (Fig. 9D). After *SIX2* transcription was

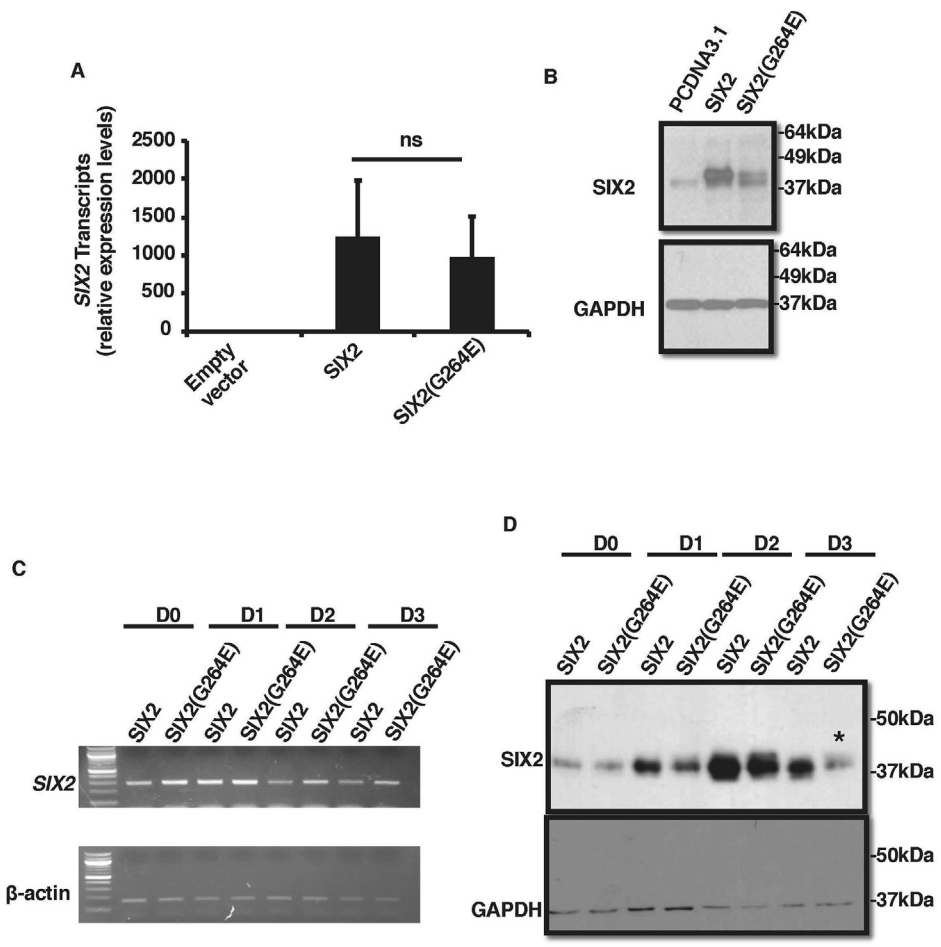

Fig. 9. The SIX2 (p.Gly264Glu) protein is unstable and degraded compared to WT. A. Empty vector, *SIX2* or *SIX2 (p.Gly264Glu)* expression plasmids were transfected into 293 T cells and after 48 h; cells were harvested for RT-qPCR. *SIX2* expression (normalized to *β-actin*) is reported. **B.** A Western blot experiment to measure SIX2 protein levels from the same conditions in A. **C.** HEK293t cells were transfected with either *SIX2* or *SIX2(G264E)* and treated with actinomycin D 24 h later (D0). RT-PCR from RNA isolated on day 0 and the following days were performed to detect *SIX2* and *β-actin* transcripts. **D.** Western blotting of SIX2 and the GAPDH proteins from the same lysates examined in C.

inhibited, degradation of the wildtype and variant peptides was observed at D3, however much less SIX2 variant protein remained on D3, confirming the SIX2 (p.Gly264Glu) is indeed more labile (see asterisk Fig. 9D).

Furthermore, the transfection of the SIX2 (p.Gly264Glu) variant resulted in less PAX9 endogenous expression compared to WT SIX2 (Fig. 7D). Thus, our results show that SIX2 can directly regulate *PAX9* expression, and this activation is compromised by the p. Gly264Glu variant.

4. Discussion

NSCL/P is one of the most common birth defects. Patients who are afflicted by these severe craniofacial defects will require multiple surgeries during the course of their development. In addition to physical adjustments, NSCL/P patients also require speech therapy and potentially other types of treatment in order to deal with the psychosocial burdens of their condition. In all, the total cost of all types of care these patients require may total well above 200,000 dollars. There are both genetic and environmental underpinnings for NSCL/P, and the identification of these factors using different technologies including GWAS, SysFACE and mouse models, is currently a hot research topic. A small number of genes have been identified so far, suggesting there are many more genes waiting to be discovered.

Mouse models are the most commonly selected animal model used to study the genetic underpinnings of NSCL/P, due to the conservation of the biological processes underlying palatogenesis in mice and humans. Previous studies have identified different requirements for the outgrowth, elevation, extension and fusion of the palate shelves; the temporospatial regulation of each of these processes is required for complete palate development. The palatine process of the maxilla and palatine bone form the anterior and posterior secondary palate, respectively. Palate shelves meet at the midline and form the medial epithelium seam (MES) at E15.5. The anterior two-thirds of the palate, which forms the hard palate, undergoes an intramembranous ossification process after E15.5. Proper timing of this process is essential for palate development; both premature and delayed bone formation on palate shelves could cause cleft palate (Baek et al., 2011; Mori-Akiyama et al., 2003). For example, the expression of *Runx2* and *Osx* transcription factors are increased in *Sox9*$^{-/-}$ embryos leading to premature ossification and clefting. Lack of osteogenesis also can cause cleft palate. In *Bmpr1a* mutant mice, there is decreased osteogenesis of the palatine process and a loss of mesenchymal condensation, causing cleft palate. Besides cell differentiation, correct cell proliferation is also important to maintain palatogenesis successfully. Sonic hedgehog (Shh) signaling is important for epithelial-mesenchymal interaction and controlling epithelial and mesenchymal cell proliferation during palatogenesis. Errors in the Shh pathway can also cause cleft palate.

A recent study showed how *Six1* and *Six2* regulate frontonasal development partly through the expression of *Alx* genes (Liu et al., 2019). *Six1* and *Six2* are expressed in the neural crest-derived frontonasal mesenchyme and a double knockout of *Six1/Six2* resembles defects in *Alx* family knockout mice (Beverdam et al., 2001; Qu et al., 1999). Furthermore, it was reported that *Six2* complements *Six1* function in maxillary and mandibular development through regulating BMP signaling (Liu et al., 2019). It is clear from these studies that both *Six1* and *Six2* are required for frontonasal development and have some redundant functions during craniofacial development.

4.1. Six2 regulates cell proliferation and a lack of Six2 causes premature ossification of the palate shelves

Cell differentiation and cell proliferation are important to maintain palatogenesis. Cell proliferation of the palatal mesenchyme drives the outgrowth of the palatal shelves that will form the roof of the oral cavity. BrdU staining at E14.5 identified a decrease in cell proliferation of the palatal shelves in *Six2*$^{-/-}$ embryos. At E16.5, the non-extended palatal shelves of *Six2*$^{-/-}$ embryos were more ossified than their WT littermates. In *Six2*$^{-/-}$ embryos, we found delays in the elevation of the palatal shelves. However, *Six2*$^{-/-}$ palate shelves were able to elevate, but much later during embryonic development. Even after *Six2*$^{-/-}$ palatal shelf elevation had completed by E16.5, palate shelf extension failed to occur. Together, the decrease in the proliferation of the palatal mesenchyme leading to a lack of palate shelf extension, combined with premature ossification, were likely responsible for the clefting observed in *Six2*$^{-/-}$ embryos and mice.

4.2. A SIX2 human variant is associated with clefting

A human variant of SIX2 was identified and associated with one family whose proband presented clinically with cleft palate. While this variant was predicted by polyphen to be benign and tolerated by sorting intolerant from tolerant (SIFT) we show that this variant caused the mutant protein to be relatively unstable compared to the WT SIX2 protein. We also speculate that this variant may affect protein interactions which decrease the transcriptional activity of the SIX2 variant. Clearly protein interactions regulate transcriptional activation and palate development as we have shown for TBX1 and PITX2 (Gao et al., 2015). While there are several human syndromic gene variants associated with clefting, this newly identified non-syndromic *SIX2* variant provides new mechanisms for the role of SIX2 and transcription factors in cleft palate morphogenesis. We note that the mother with the variant does not have overt clefts. This is not surprising, and it is very possible that the mother has a subclinical form of cleft only observable using advanced imaging techniques (Neiswanger et al., 2007). Another consideration is that the cleft phenotype observed in the child could be the outcome of genetic risk shared with the mother combined with environmental exposures during the periconceptional period (Little et al., 2004). Interestingly, the low penetrance of clefting observed in humans correlates with the low penetrance we observed in the *Six2* null embryos. The low penetrance of the clefting phenotype in the *Six2* null mice could also be due to the expression of *Six1* as they have overlapping expression domains and function (Liu et al., 2019).

4.3. Six2 regulates Pax9 expression

Pax9 has been identified as an essential master regulator of palate development in humans, and also in mice (Ichikawa et al., 2006; Jia et al., 2017). When *Pax9* is ablated in the developing mouse embryonic palate shelves, defects in palate shelf elevation and elongation are observed, resulting in the loss of palatal fusion (Zhou et al., 2013). Interestingly, these are the same defects we characterized in *Six2*$^{-/-}$ embryos. *Pax9* is expressed in the developing palate epithelium and mesenchyme, and is therefore partially colocalized with Six2 (Zhou et al., 2013). Pax9 has been demonstrated to interact with many different mesenchymal transcription factors and signaling pathways required for palate development such as Wnt, β-catenin, Msx1, Osr2, Bmp4, Fgf10, and Fgf8 to regulate cell differentiation and cell proliferation during palatogenesis. (Hilliard et al., 2005; Ichikawa et al., 2006; Jia et al., 2017; Zhou et al., 2013). Our work contributes to this understanding by uncovering a *Six2-Pax9* axis that regulates the proliferation and differentiation of the palatal mesenchyme during the process. Six2 directly regulates *PAX9* expression. Disrupting this axis results in cleft palate due to the failure of palate shelf extension, an outcome resultant of the loss of cell proliferation and premature ossification.

Declaration of competing interest

The authors have no conflicts of interest to report.

Acknowledgments

We thank members of the Amendt laboratory for helpful discussions, Christine Blaumueller for editorial expertise and the Carver Trust for support of the microCT scanner. We thank Dr. Rulang Jiang for sharing unpublished data and critical comments. This research project was support by funds from the University of Iowa Carver College of Medicine and College of Dentistry and NIDCR grants R03DE024776 to S.L., I.S.; R01DE026172 to I.S.; DE026433 to B.A.A and DE023520 to B.A.A.

Appendix A. Supplementary data

Supplementary data to this article can be found online at https://doi.org/10.1016/j.ydbio.2019.11.010.

References

Adzhubei, I.A., Schmidt, S., Peshkin, L., Ramensky, V.E., Gerasimova, A., Bork, P., Kondrashov, A.S., Sunyaev, S.R., 2010. A method and server for predicting damaging missense mutations. Nat. Methods 7, 248–249.

Anand, D., Kakrana, A., Siddam, A.D., Huang, H., Saadi, I., Lachke, S.A., 2018. RNA sequencing-based transcriptomic profiles of embryonic lens development for cataract gene discovery. Hum. Genet. 137, 941–954.

Baek, J.-A., Lan, Y., Liu, H., Maltby, K.M., Mishina, Y., Jiang, R., 2011. Bmpr1a signaling plays critical roles in palatal shelf growth and palatal bone formation. Dev. Biol. 350, 520–531.

Beaty, T.H., Murray, J.C., Marazita, M.L., Munger, R.G., Ruczinski, I., Hetmanski, J.B., Liang, K.Y., Wu, T., Murray, T., Fallin, M.D., Redett, R.A., Raymond, G., Schwender, H., Jin, S.-C., Cooper, M.E., Dunnwald, M., Mansilla, M.A., Leslie, E., Bullard, S., Lidral, A.C., Moreno, L.M., Menezes, R., Vieira, A.R., Petrin, A., Wilcox, A.J., 2010. A genome-wide association study of cleft lip with and without cleft palate identifies risk variants near MAFB and ABCA4. Nat. Genet. 42, 525–529.

Beverdam, A., Brouwer, A., Reijnen, M., Korving, J., Meijlink, F., 2001. Severe nasal clefting and abnormal embryonic apoptosis in Alx3/Alx4 double mutant mice. Development 128, 3975–3986.

Birnbaum, S., Ludwig, K.U., Reutter, H., Herms, S., Steffens, M., Rubini, M., Baluardo, C., Ferrian, M., Almeida de Assis, N., Alblas, M.A., Barth, S., Freudenberg, J., Lauster, C., Schmidt, G., Scheer, M., Braumann, B., Berge, S.J., Reich, R.H., Schiefke, F., Hemprich, A., Potzsch, S., Steegers-Theunissen, R.P., Potzsch, B., Moebus, S., Horsthemke, B., Kramer, F.J., Wienker, T.F., Mossey, P.A., Propping, P., Cichon, S., Hoffmann, P., Knapp, M., Nothen, M.M., Mangold, E., 2009. Key susceptibility locus for nonsyndromic cleft lip with or without cleft palate on chromosome 8q24. Nat. Genet. 41, 473–477.

Brodbeck, S., Besenbeck, B., Englert, C., 2004. The transcription factor Six2 activates expression of the Gdnf gene as well as its own promoter. Mech. Dev. 121, 1211–1222.

Bush, J.O., Jiang, R., 2012. Palatogenesis: morphogenetic and molecular mechanisms of secondary palate development. Development 139, 231–243.

Butali, A., Mossey, P.A., Adeyemo, W.L., Eshete, M.A., Gowans, L.J.J., Busch, T.D., Jain, D., Yu, W., Huan, L., Laurie, C.A., Laurie, C.C., Nelson, S., Li, M., Sanchez-Lara, P.A., Magee 3rd, W.P., Magee, K.S., Auslander, A., Brindopke, F., Kay, D.M., Caggana, M., Romitti, P.A., Mills, J.L., Audu, R., Onwuamah, C., Oseni, G.O., Owais, A., James, O., Olaitan, P.B., Aregbesola, B.S., Braimah, R.O., Oginni, F.O., Oladele, A.O., Bello, S.A., Rhodes, J., Shiang, R., Donkor, P., Obiri-Yeboah, S., Arthur, F.K.N., Twumasi, P., Agbenorku, P., Plange-Rhule, G., Oti, A.A., Ogunlewe, O.M., Oladega, A.A., Adekunle, A.A., Erinoso, A.O., Adamson, O.O., Elufowoju, A.A., Ayelomi, O.I., Hailu, T., Hailu, A., Demissie, Y., Derebew, M., Eliason, S., Romero-Bustillous, M., Lo, C., Park, J., Desai, S., Mohammed, M., Abate, F., Abdur-Rahman, L.O., Anand, D., Saadi, I., Oladugba, A.V., Lachke, S.A., Amendt, B.A., Rotimi, C.N., Marazita, M.L., Cornell, R.A., Murray, J.C., Adeyemo, A.A., 2018. Genomic analyses in african populations identify novel risk loci for cleft palate. Hum. Mol. Genet. 28, 1038–1051. PMCID:PMC6400042.

Conway, J.C., Taub, P.J., Kling, R., Oberoi, K., Doucette, J., Jabs, E.W., 2015. Ten-year experience of more than 35,000 orofacial clefts in Africa. BMC Pediatr. 15, 8.

Cox, L.L., Cox, T.C., Moreno Uribe, L.M., Zhu, Y., Richter, C.T., Nidey, N., Standley, J.M., Deng, M., Blue, E., Chong, J.X., Yang, Y., Carstens, R.P., Anand, D., Lachke, S.A., Smith, J.D., Dorschner, M.O., Bedell, B., Kirk, E., Hing, A.V., Venselaar, H., Valencia-Ramirez, L.C., Bamshad, M.J., Glass, I.A., Cooper, J.A., Haan, E., Nickerson, D.A., van Bokhoven, H., Zhou, H., Krahn, K.N., Buckley, M.F., Murray, J.C., Lidral, A.C., Roscioli, T., 2018. Mutations in the epithelial cadherin-p120-catenin complex cause mendelian non-syndromic cleft lip with or without cleft palate. Am. J. Hum. Genet. 102, 1143–1157.

Dixon, M.J., Marazita, M.L., Beaty, T.H., Murray, J.C., 2011. Cleft lip and palate: understanding genetic and environmental influences. Nat. Rev. Genet. 12, 167–178.

Gao, S., Moreno, M., Eliason, S., Cao, H., Li, X., Yu, W., Bidlack, F.B., Margolis, H.C., Baldini, A., Amendt, B.A., 2015. TBX1 protein interactions and microRNA-96-5p

regulation controls cell proliferation during craniofacial and dental development: implications for 22q11.2 deletion syndrome. Hum. Mol. Genet. 24, 2330–2348.
Grant, S.F., Wang, K., Zhang, H., Glaberson, W., Annaiah, K., Kim, C.E., Bradfield, J.P., Glessner, J.T., Thomas, K.A., Garris, M., Frackelton, E.C., Otieno, F.G., Chiavacci, R.M., Nah, H.D., Kirschner, R.E., Hakonarson, H., 2009. A genome-wide association study identifies a locus for nonsyndromic cleft lip with or without cleft palate on 8q24. J. Pediatr. 155, 909–913.
He, G., Tavella, S., Hanley, K.P., Self, M., Oliver, G., Grifone, R., Hanley, N., Ward, C., Bobola, N., 2010. Inactivation of Six2 in mouse identifies a novel genetic mechanism controlling development and growth of the cranial base. Dev. Biol. 344, 720–730.
Hilliard, S.A., Yu, L., Gu, S., Zhang, Z., Chen, Y.P., 2005. Regional regulation of palatal growth and patterning along the anterior-posterior axis in mice. J. Anat. 207, 655–667.
Hufnagel, R.B., Zimmerman, S.L., Krueger, L.A., Bender, P.L., Ahmed, Z.M., Saal, H.M., 2016. A new frontonasal dysplasia syndrome associated with deletion of the SIX2 gene. Am. J. Med. Genet. Part A 170a, 487–491.
Ichikawa, E., Watanabe, A., Nakano, Y., Akita, S., Hirano, A., Kinoshita, A., Kondo, S., Kishino, T., Uchiyama, T., Niikawa, N., Yoshiura, K., 2006. PAX9 and TGFB3 are linked to susceptibility to nonsyndromic cleft lip with or without cleft palate in the Japanese: population-based and family-based candidate gene analyses. J. Hum. Genet. 51, 38–46.
Jia, S., Zhou, J., Fanelli, C., Wee, Y., Bonds, J., Schneider, P., Mues, G., D'Souza, R.N., 2017. Small-molecule Wnt agonists correct cleft palates in Pax9 mutant mice in utero. Development 144, 3819–3828.
Kakrana, A., Yang, A., Anand, D., Djordjevic, D., Ramachandruni, D., Singh, A., Huang, H., Ho, J.W.K., Lachke, S.A., 2018. iSyTE 2.0: a database for expression-based gene discovery in the eye. Nucleic Acids Res. 46, D875–d885.
Kawakami, K., Ohto, H., Takizawa, T., Saito, T., 1996. Identification and expression of six family genes in mouse retina. FEBS Lett. 393, 259–263.
Kist, R., Watson, M., Wang, X., Cairns, P., Miles, C., Reid, D.J., Peters, H., 2005. Reduction of Pax9 gene dosage in an allelic series of mouse mutants causes hypodontia and oligodontia. Hum. Mol. Genet. 14, 3605–3617.
Kumar, P., Henikoff, S., Ng, P.C., 2009. Predicting the effects of coding non-synonymous variants on protein function using the SIFT algorithm. Nat. Protoc. 4, 1073–1081.
Lachke, S.A., Ho, J.W., Kryukov, G.V., O'Connell, D.J., Aboukhalil, A., Bulyk, M.L., Park, P.J., Maas, R.L., 2012. iSyTE: integrated Systems Tool for Eye gene discovery. Investig. Ophthalmol. Vis. Sci. 53, 1617–1627.
Leslie, E.J., Carlson, J.C., Cooper, M.E., Christensen, K., Weinberg, S.M., Marazita, M.L., 2017. Exploring subclinical phenotypic features in twin pairs discordant for cleft lip and palate. Cleft Palate-Craniofacial J. 54, 90–93.
Leslie, E.J., Liu, H., Carlson, J.C., Shaffer, J.R., Feingold, E., Wehby, G., Laurie, C.A., Jain, D., Laurie, C.C., Doheny, K.F., McHenry, T., Resick, J., Sanchez, C., Jacobs, J., Emanuele, B., Vieira, A.R., Neiswanger, K., Standley, J., Czeizel, A.E., Deleyiannis, F., Christensen, K., Munger, R.G., Lie, R.T., Wilcox, A., Romitti, P.A., Field, L.L., Padilla, C.D., Cutiongco-de la Paz, E.M.C., Lidral, A.C., Valencia-Ramirez, L.C., Lopez-Palacio, A.M., Valencia, D.R., Arcos-Burgos, M., Castilla, E.E., Mereb, J.C., Poletta, F.A., Orioli, I.M., Carvalho, F.M., Hecht, J.T., Blanton, S.H., Buxó, C.J., Butali, A., Mossey, P.A., Adeyemo, W.L., James, O., Braimah, R.O., Aregbesola, B.S., Eshete, M.A., Deribew, M., Koruyucu, M., Seymen, F., Ma, L., de Salamanca, J.E., Weinberg, S.M., Moreno, L., Cornell, R.A., Murray, J.C., Marazita, M.L., 2016. A genome-wide association study of nonsyndromic cleft palate identifies an etiologic missense variant in GRHL3. Am. J. Hum. Genet. 98, 744–754.
Leslie, E.J., Taub, M.A., Liu, H., Steinberg, K.M., Koboldt, D.C., Zhang, Q., Carlson, J.C., Hetmanski, J.B., Wang, H., Larson, D.E., Fulton, R.S., Kousa, Y.A., Fakhouri, W.D., Naji, A., Ruczinski, I., Begum, F., Parker, M.M., Busch, T., Standley, J., Rigdon, J., Hecht, J.T., Scott, A.F., Wehby, G.L., Christensen, K., Czeizel, A.E., Deleyiannis, F.W., Schutte, B.C., Wilson, R.K., Cornell, R.A., Lidral, A.C., Weinstock, G.M., Beaty, T.H., Marazita, M.L., Murray, J.C., 2015. Identification of functional variants for cleft lip with or without cleft palate in or near PAX7, FGFR2, and NOG by targeted sequencing of GWAS loci. Am. J. Hum. Genet. 96, 397–411.
Little, J., Cardy, A., Arslan, M.T., Gilmour, M., Mossey, P.A., 2004. Smoking and orofacial clefts: a United Kingdom-based case-control study. Cleft Palate-Craniofacial J. 41, 381–386.
Liu, H., Leslie, E.J., Carlson, J.C., Beaty, T.H., Marazita, M.L., Lidral, A.C., Cornell, R.A., 2017. Identification of common non-coding variants at 1p22 that are functional for non-syndromic orofacial clefting. Nat. Commun. 8, 14759.
Liu, Z., Li, C., Xu, J., Lan, Y., Liu, H., Li, X., Maire, P., Wang, X., Jiang, R., 2019. Crucial and overlapping roles of Six1 and Six2 in craniofacial development. J. Dent. Res. 98, 572–579.
Ludwig, K.U., Mangold, E., Herms, S., Nowak, S., Reutter, H., Paul, A., Becker, J., Herberz, R., AlChawa, T., Nasser, E., Bohmer, A.C., Mattheisen, M., Alblas, M.A., Barth, S., Kluck, N., Lauster, C., Braumann, B., Reich, R.H., Hemprich, A., Potzsch, S., Blaumeiser, B., Daratsianos, N., Kreusch, T., Murray, J.C., Marazita, M.L., Ruczinski, I., Scott, A.F., Beaty, T.H., Kramer, F.-J., ienker, T.F., Steegers-Theunissen, R.P., Rubini, M., Mossey, P.A., Hoffmann, P., Lange, C., Cichon, S., Propping, P., Knapp, M., Nothen, M.M., 2012. Genome-wide meta-analyses of nonsyndromic cleft lip with or without cleft palate identify six new risk loci. Nat. Genet. 44, 968–971.
Mangold, E., Ludwig, K.U., Birnbaum, S., Baluardo, C., Ferrian, M., Herms, S., Reutter, H., de Assis, N.A., Chawa, T.A., Mattheisen, M., Steffens, M., Barth, S., Kluck, N., Paul, A., Becker, J., Lauster, C., Schmidt, G., Braumann, B., Scheer, M., Reich, R.H., Hemprich, A., Potzsch, S., Blaumeiser, B., Moebus, S., Krawczak, M., Schreiber, S., Meitinger, T., Wichmann, H.E., Steegers-Theunissen, R.P., Kramer, F.J., Cichon, S., Propping, P., Wienker, T.F., Knapp, M., Rubini, M., Mossey, P.A., Hoffmann, P., Nothen, M.M., 2010. Genome-wide association study identifies two susceptibility loci for nonsyndromic cleft lip with or without cleft palate. Nat. Genet. 42, 24–26.
Mori-Akiyama, Y., Akiyama, H., Rowitch, D.H., B., d.C., 2003. Sox9 is required for determination of the chondrogenic cell lineage in the cranial neural crest. Proc. Natl. Acad. Sci. U. S. A. 100, 9360–9365.
Neiswanger, K., Weinberg, S.M., Rogers, C.R., Brandon, C.A., Cooper, M.E., Bardi, K.M., Deleyiannis, F.W., Resick, J.M., Bowen, A., Mooney, M.P., de Salamanca, J.E., Gonzalez, B., Maher, B.S., Martin, R.A., Marazita, M.L., 2007. Orbicularis oris muscle defects as an expanded phenotypic feature in nonsyndromic cleft lip with or without cleft palate. Am. J. Med. Genet. Part A 143a, 1143–1149.
Nonomura, K., Takahashi, M., Wakamatsu, Y., Takano-Yamamoto, T., Osumi, N., 2010. Dynamic expression of Six family genes in the dental mesenchyme and the epithelial ameloblast stem/progenitor cells during murine tooth development. J. Anat. 216, 80–91.
O'Brien, L.L., Guo, Q., Lee, Y., Tran, T., Benazet, J.D., Whitney, P.H., Valouev, A., McMahon, A.P., 2016. Differential regulation of mouse and human nephron progenitors by the Six family of transcriptional regulators. Development 143, 595–608.
Okello, D.O., Iyyanar, P.P.R., Kulyk, W.M., Smith, T.M., Lozanoff, S., Ji, S., Nazarali, A.J., 2017. Six2 plays an intrinsic role in regulating proliferation of mesenchymal cells in the developing palate. Front. Physiol. 8, 955.
Park, J.S., Ma, W., O'Brien, L.L., Chung, E., Guo, J.J., Cheng, J.G., Valerius, M.T., McMahon, J.A., Wong, W.H., McMahon, A.P., 2012. Six2 and Wnt regulate self-renewal and commitment of nephron progenitors through shared gene regulatory networks. Dev. Cell 23, 637–651.
Peters, H., Neubuser, A., Kratochwil, K., Balling, R., 1998. Pax9-deficient mice lack pharyngeal pouch derivatives and teeth and exhibit craniofacial and limb abnormalities. Genes Dev. 12, 2735–2747.
Qu, S., Tucker, S.C., Zhao, Q., deCrombrugghe, B., Wisdom, R., 1999. Physical and genetic interactions between Alx4 and Cart 1. Development 126, 359–369.
Rahimov, F., Marazita, M.L., Visel, A., Cooper, M.E., Hitchler, M.J., Rubini, M., Domann, F.E., Govil, M., Christensen, K., Bille, C., Melbye, M., Jugessur, A., Lie, R.T., Wilcox, A.J., Fitzpatrick, D.R., Green, E.D., Mossey, P.A., Little, J., Steegers-Theunissen, R.P., Pennacchio, L.A., Schutte, B.C., Murray, J.C., 2008. Disruption of an AP-2 alpha binding site in an IRF6 enhancer is associated with cleft lip. Nat. Genet. 40, 1341–1347.
Self, M., Lagutin, O.V., Bowling, B., Hendrix, J., Cai, Y., Dressler, G.R., Oliver, G., 2006. Six2 is required for suppression of nephrogenesis and progenitor renewal in the developing kidney. EMBO J. 25, 5214–5228.
Stuppia, L., Capogreco, M., Marzo, G., La Rovere, D., Antonucci, I., Gatta, V., Palka, G., Mortellaro, C., Tete, S., 2011. Genetics of syndromic and nonsyndromic cleft lip and palate. J. Craniofac. Surg. 22, 1722–1726.
Sun, Y., Huang, Y., Yin, A., Pan, Y., Wang, Y., Wang, C., Du, Y., Wang, M., Lan, F., Hu, Z., Wang, G., Jiang, M., Ma, J., Zhang, X., Ma, H., Ma, J., Zhang, W., Huang, Q., Zhou, Z., Ma, L., Li, Y., Jiang, H., Xie, L., Jiang, Y., Shi, B., Cheng, J., Shen, H., Wang, L., Yang, Y., 2015. Genome-wide association study identifies a new susceptibility locus for cleft lip with or without a cleft palate. Nat. Commun. 6, 6414.
Sun, Z., Yu, W., Navarro, M.S., Sweat, M., Eliason, S., Sharp, T., Liu, H., Seidel, K., Zhang, L., Moreno, M., Lynch, T., Holton, N.E., Rogers, L., Neff, T., Goodheart, M.J., Michon, F., Klein, O.D., Chai, Y., Dupuy, A., Engelhardt, J.F., Chen, Z., Amendt, B.A., 2016. Sox 2 and Lef-1 interact with Pitx2 to regulate incisor development and stem cell renewal. Development 143, 4115–4126.
Venselaar, H., Te Beek, T.A., Kuipers, R.K., Hekkelman, M.L., Vriend, G., 2010. Protein structure analysis of mutations causing inheritable diseases. An e-Science approach with life scientist friendly interfaces. BMC Bioinf. 11, 548.
Wolf, Z.T., Brand, H.A., Shaffer, J.R., Leslie, E.J., Arzi, B., Willet, C.E., Cox, T.C., McHenry, T., Narayan, N., Feingold, E., Wang, X., Sliskovic, S., Karmi, N., Safra, N., Sanchez, C., Deleyiannis, F.W.B., Murray, J.C., Wade, C.M., Marazita, M.L., Bannasch, D.L., 2015. Genome-Wide association studies in dogs and humans identify ADAMTS20 as a risk variant for cleft lip and palate. PLoS Genet. 11, e1005059.
Yu, Y., Zuo, X., He, M., Gao, J., Fu, Y., Qin, C., Meng, L., Wang, W., Song, Y., Cheng, Y., Zhou, F., Chen, G., Zheng, X., Wang, X., Liang, B., Zhu, Z., Fu, X., Sheng, Y., Hao, J., Liu, Z., Yan, H., Mangold, E., Ruczinski, I., Liu, J., Marazita, M.L., Ludwig, K.U., Beaty, T.H., Zhang, X., Sun, L., Bian, Z., 2017. Genome-wide analyses of non-syndromic cleft lip with palate identify 14 novel loci and genetic heterogeneity. Nat. Commun. 8, 14364.
Zhang, J., Yang, R., Liu, Z., Hou, C., Zong, W., Zhang, A., Sun, X., Gao, J., 2015. Loss of lysyl oxidase-like 3 causes cleft palate and spinal deformity in mice. Hum. Mol. Genet. 24, 6174–6185.
Zhou, J., Gao, Y., Lan, Y., Jia, S., Jiang, R., 2013. Pax9 regulates a molecular network involving Bmp4, Fgf10, Shh signaling and the Osr2 transcription factor to control palate morphogenesis. Development 140, 4709–4718.